Dynamical Charge Tensors and Infrared Spectrum of Amorphous SiO_2

Alfredo Pasquarello and Roberto Car

Institut Romand de Recherche Numérique en Physique des Matériaux (IRRMA), Ecublens, CH-1015 Lausanne, Switzerland, and Département de la Matière Condensée, Université de Genève, 24 Quai E. Ansermet, CH-1211 Geneva, Switzerland

(Received 20 March 1997)

Using a model structure consisting of a network of corner sharing tetrahedra, we calculate the infrared spectrum of amorphous SiO_2 within a first-principles approach and find good agreement with experiment both for the positions and the intensities of the main peaks. In addition to the vibrational properties, this required the dynamical charge tensors, which were obtained applying the recent quantum polarization theory. The relative intensities in the spectrum depend sensitively on the charge tensors and their anisotropic components are crucial to obtain good agreement with experiment. We find that the Born charges can be correlated to the local structural properties. [S0031-9007(97)03891-X]

PACS numbers: 78.30.Ly, 63.50.+x

Infrared spectroscopy is one of the most valuable experimental techniques to access the vibrational properties of amorphous silicon dioxide (a-SiO_2) [1–6]. The understanding of these properties constitutes a critical step towards the assessment of a definite structural model for a-SiO_2. Furthermore, there is a technological interest in the infrared coupling intensities because they affect the loss functions in optical fibers.

It has been common practice to assume the breakdown of selection rules in glassy a-SiO_2 and to interpret spectroscopic features in terms of the vibrational density of states. This indeed applies for inelastic neutron spectra [7,8] because the scattering lengths of Si and O are comparable. However, when the long-wavelength limit is probed as in infrared [1–6] or Raman [2,3] experiments, the principal spectroscopic features do not resemble the vibrational density of states and their interpretation must rely on the coupling intensities.

Both infrared and Raman spectra appear to be dominated by the occurrence of longitudinal-optic transverse-optic (LO-TO) splittings [2,3,5,6,9]. However, hyper-Raman experiments showed that LO-TO excitations are observed at close but distinct frequencies with respect to Raman features, suggesting that the latter are sensitive to a different set of vibrational modes [10,11]. Therefore, in order to identify the active modes, it is critical to accurately situate the main optical excitations with respect to the features in the vibrational density of states.

So far the interpretation of infrared spectra of disordered systems strongly relied on classical molecular dynamics techniques. The most recent developments of these methods [12] included polarization effects and produced spectra in which the frequencies of the main features are in good agreement with experiment. However, a correct distribution of the intensities throughout the spectrum appears more difficult to achieve within these approaches.

An accurate calculation of infrared intensities of glassy materials is generally not trivial and requires several ingredients. These include a good structural model, the complete description of the vibrational properties, and the dynamical Born charge tensors. Dynamical charges are routinely evaluated for crystalline systems [13]. By contrast, when the periodicity is lost as in an amorphous system, the charge tensors of all the atoms in the model differ and their calculation in such a case has not been attempted so far. Whereas classical potentials can successfully be used for determining structural [14] and even dynamical properties [12,15–17], the effective Born charges can only be obtained within a theory which explicitly treats the electronic structure.

In this Letter, we calculate the infrared absorption spectrum of amorphous SiO_2 from first principles. We adopt a structural model which consists of a network of corner sharing tetrahedra, previously obtained [18] using quantum molecular dynamics [19,20]. The structural and vibrational properties of this model have already been shown to be in excellent agreement with elastic and inelastic neutron measurements [8,18]. In order to access the dynamical charge tensors, we applied the recently developed polarization theory based on geometric quantum phase concepts [13,21]. The calculated absorption spectra present peaks and relative intensities in very good agreement with experiment. We evaluate the role of the anisotropic components of the Born charge tensors, usually disregarded in semiempirical calculations, and find that their neglect sensitively affects the relative intensities in the spectrum. Furthermore, our analysis shows that the dynamical charges correlate with the local structural properties, suggesting a way to assign Born charges when they are unavailable.

The calculations are performed within density functional theory, using the local density approximation for the exchange and correlation energy [22]. The model structure [18] used in the present study contained 72 atoms, fully relaxed at the experimental density ($2.20\ g/cm^3$) in a periodically repeated cubic cell. Only the valence electrons were explicitly retained in our calculation using pseudopotentials (PPs) to account for

 0031-9007/97/79(9)/1766(4)$10.00

core-valence interactions. We used a norm-conserving PP for Si [23] and an ultrasoft PP for O [24]. The electronic wave functions and charge density were described by plane wave basis sets with cutoffs of 24 and 200 Ry, respectively. The Brillouin zone of the cell was sampled only at the Γ point. A detailed description of the method is given in Ref. [20]. We made use of the vibrational properties calculated in Ref. [8], where the dynamical matrix was calculated numerically by taking finite differences of the atomic forces. The vibrational frequencies ω_n and their corresponding normalized eigenmodes ξ_n could then be derived by diagonalization.

The electronic contribution to the effective Born charge tensor of a given atom I is defined in terms of the derivative of the polarization $\mathbf{P}$ with respect to a displacement $\mathbf{u}$ of that atom [13]:

$$Z^{e*}_{ij}(I) = \frac{\Omega}{e} \frac{\partial P_i}{\partial u_j}, \tag{1}$$

where $\Omega = L^3$ is the volume of the cell. The polarization can be expressed in terms of geometric quantum phases γ_i, for $i = x, y, z$ [13,21]: $P_i = (e/\pi L^2)\gamma_i$. The phases γ_i, also known as Berry phases [25], are a property of the electronic wave functions and can be evaluated for finite displacements of the atoms [26,27]. Using Eq. (1), the charge tensors Z^* for every atom can thus be obtained. We used atomic displacements of ± 0.1 bohr which fall within a regime in which the polarization depends linearly on the displacements, and checked that the acoustic sum rule $\sum_I Z^*_{ij}(I) = 0$ was verified within 0.07 electronic charge units.

The charge tensors can be decomposed according to the representations of the spatial rotations. The isotropic part ($l = 0$) is given by $Z^*_0 \delta_{ij}$ and has the same trace as Z^*, whereas the $l = 1$ and $l = 2$ anisotropic parts correspond to the antisymmetric and to the traceless symmetric decomposition of Z^*_{ij}, respectively. By adopting the standard matricial norm, this decomposition can be quantified (Table I). The isotropic contribution to the charge tensors is by far the dominant one. The only non-negligible anisotropic component is the $l = 2$ contribution for the O atoms, which are the most polarizable atoms in this system. Comparison to the values for α quartz [28] shows a close correspondence indicating that the bonding properties in the two systems are very similar [29].

TABLE I. Average isotropic Born charges, the width of their distribution, and the average contribution of isotropic ($l = 0$) and anisotropic ($l = 1$ and $l = 2$) components to the charge tensors, for a-SiO_2 and α quartz [28].

	a-SiO_2		α quartz	
	Oxygen	Silicon	Oxygen	Silicon
$\langle Z^*_0 \rangle$	−1.588	3.177	−1.684	3.368
ΔZ^*_0	0.078	0.121	...	...
$l = 0$	82.27%	96.94%	82.87%	98.88%
$l = 1$	0.16%	0.46%	0.05%	0.53%
$l = 2$	17.56%	2.60%	17.08%	0.59%

The isotropic Born charges of our amorphous model are distributed around a most probable value with no particular structure in the distribution. This is consistent with the network model, in which the disorder is principally given by a broad distribution of Si-O-Si bond angles. The average and the width of the Si and O isotropic charge distributions are given in Table I. Compared to α quartz [28], the average isotropic charges in a-SiO_2 are found to be a little smaller. This can be understood by relating the isotropic charges to the local structural properties. We display in Fig. 1(a) the isotropic O charge vs the Si-O-Si bond angle. This reveals the existence of a correlation between these two quantities. The dynamical charges increase with increasing bond angles, reflecting the variation in ionic character. This also explains the larger negative O charge in α quartz, where the Si-O-Si bond angle is 143.7°, significantly larger than the average bond angle in our model (136.9°). We also found an unexpected correlation for the Si isotropic charge with an effective neutralizing charge, defined as the opposite of the half sum of the isotropic charges of the four neighboring O atoms [Fig. 1(b)]. This indicates that a dynamical charge neutrality condition is approximately satisfied locally [30], i.e., within every tetrahedral subunit. Overall, these considerations indicate that the Born charge tensors in a-SiO_2 depend on the local structure and suggest that their values could be extracted by studying systems of small size.

We now have all the ingredients to calculate the imaginary part of the transverse dielectric response function in the long wavelength limit [9,31]:

$$\mathrm{Im}\ \epsilon_\perp(\omega) = \frac{4\pi}{3\Omega} \sum_n \frac{|\mathbf{F}^n|^2}{\omega^2 - \omega_n^2}, \tag{2}$$

$$F^n_k = \sum_I \sum_i Z_{ki}(I) \frac{\xi_n(I,i)}{\sqrt{m_I}}, \tag{3}$$

where I runs over the atoms, and $i = x, y, z$. The spectrum is shown in Fig. 2 together with the vibrational density of states [8]. The principal features are indicated

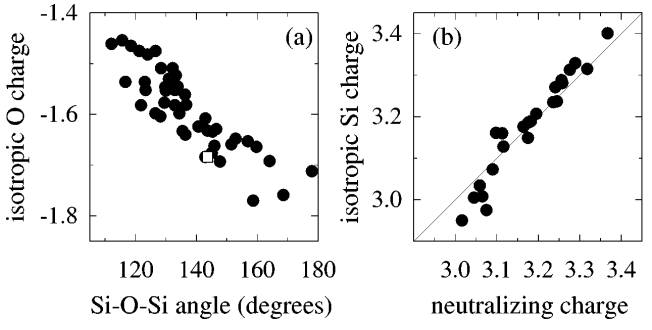

FIG. 1. (a) Isotropic O charge vs the Si-O-Si angle (the square is for α quartz [28]). (b) Isotropic Si charge vs the neutralizing charge (see text).

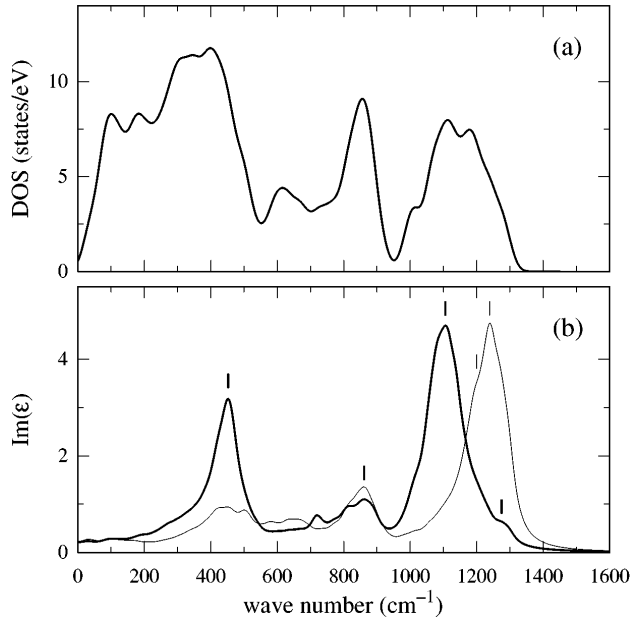

FIG. 2. (a) Vibrational density of states of a-SiO_2. (b) Im $\epsilon_\perp$ (thick) at $\mathbf{q} = 0$ and Im $\epsilon_\parallel$ (thin) at the shortest wave vector allowed by the periodic cell. A broadening of 20 cm^{-1} was used.

and their positions are reported in Table II, together with the experimental values measured by Kirk [5]. The agreement can be considered very good showing errors of about 50 cm^{-1} or less for the main peaks at about 450, 800, and 1100 cm^{-1}, and of 75 cm^{-1} for the shoulder at about 1200 cm^{-1}. Furthermore, the relative intensities of the peaks, which are known to be a rather delicate property [12], are also in good agreement with experiment (see also Fig. 3). The coupling strengths of Eq. (3) provide a measure for

$$\Delta\epsilon = \epsilon_0 - \epsilon_\infty = \frac{4\pi}{3\Omega} \sum_n \frac{|\mathbf{F}^n|^2}{\omega_n^2} . \tag{4}$$

We find $\Delta\epsilon = 1.6$ in fair agreement with the experimental value of 1.2 ($\epsilon_\infty^{\text{exp}} = 2.1$, $\epsilon_0^{\text{exp}} = 3.3$).

The two highest peaks in the transverse spectrum, the intense peak at 1106, and the weaker one at 861 cm^{-1} are related to Si-O stretching modes [32,33]. These vibrations correspond to modes of the tetrahedral subunits, in which two O atoms move closer to the central Si atom, whereas the two other ones move away [8,12]. In order

TABLE II. Peak and shoulder wave numbers (in cm^{-1}) indicated in Fig. 2, compared to experiment [5].

Theory		Experiment	
Trans.	Long.	Trans.	Long.
1106	[1239]	1076	1256
1275	[1200]	1200	1160
861		810	820
453		457	507

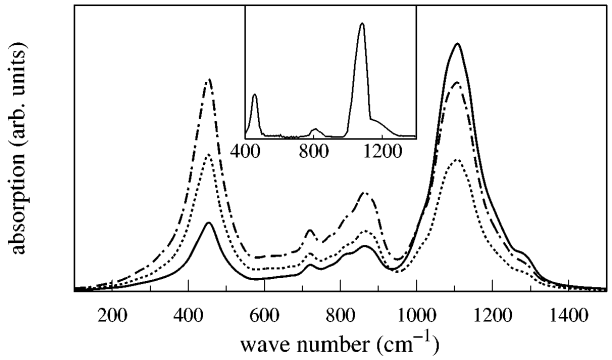

FIG. 3. Infrared absorption spectrum $\alpha(\omega) \sim \omega$ Im $\epsilon_\perp(\omega)$ calculated (a) with the full charge tensors (solid line), (b) with isotropic tensors (dotted line), or (c) with nominal point charges (dash-dotted line). Inset: experiment from Ref. [5]

to keep the center of mass immobile the central Si atom participates in these modes, contributing significantly to the peak at 861 cm^{-1} [8]. The lowest infrared peak at 453 cm^{-1} arises mainly from rocking modes in which the O atoms move perpendicular to the Si-O-Si planes [15]. The peaks in the vibrational density of states at 1180 and 615 cm^{-1} mainly correspond to O breathing modes within the tetrahedral subunits and to O bond-bending motions in the Si-O-Si plane along the bisector of the Si-O-Si angle, respectively. These vibrational modes do not show signatures in the infrared spectrum.

The splitting of the feature at about 800 cm^{-1} and the additional weak feature which appears at 721 cm^{-1} do not appear to have experimental counterparts at ambient pressure. However, at relatively low pressures ($\sim$10 kbar) these signatures are distinctly observable [4]. This might indicate that the model structure in our calculations is under a weak compression.

We estimate the imaginary part of the longitudinal dielectric response function in the long-wavelength limit by calculating [9]

$$\text{Im } \epsilon_\parallel(\mathbf{q}, \omega) = \frac{4\pi}{\Omega} \sum_n \sum_{I,J} \frac{G^n(\mathbf{q}, I) G^n(\mathbf{q}, J)}{\omega^2 - \omega_n^2} e^{i\mathbf{q}\cdot(\mathbf{R}_I - \mathbf{R}_J)}, \tag{5}$$

$$G^n(\mathbf{q}, I) = \sum_{ij} q_i Z_{ij}^*(I) \frac{\xi_n(I, j)}{\sqrt{m_I}} , \tag{6}$$

for the shortest wave vector $\mathbf{q}$ allowed by the cell periodicity [34]. The spectrum is shown in Fig. 2 and the positions of the high-frequency features are reported in Table II. Comparison with infrared absorption measurements [5] shows that the positions of the high-frequency features and the overall shape of the spectrum correspond closely. In the low-frequency region of the spectrum, where the vibrational modes are more delocalized, larger differences between the spectrum at finite wave vector and its long-wavelength limit are expected.

Since the full charge tensors are not always available, it is of interest to determine whether accurate infrared

intensities can also be obtained within simplified schemes. When nominal point charges are used, namely, -2 for O and $+4$ for Si, the intensities of the absorption peaks are significantly altered (Fig. 3), in particular, the one at 453 cm^{-1} [12]. By retaining for every atom only the isotropic component of its charge tensor, an overall decrease of the intensities is observed, but the relative intensities are not improved. In order to recover the experimentally observed shape with a dominant weight in the high-frequency peak, it is necessary to consider the anisotropic components of the charge tensors. However, it is sufficient to add the $l = 2$ anisotropic component for the O atoms, i.e., the only remaining significant contribution (Table I), to obtain a spectrum which is virtually identical to that obtained with the full charge tensors [35].

In conclusion, not only the positions of the principal peaks, but also more detailed properties, such as their relative intensities and the shape of the high-frequency features, are consistent with the structural model for a-SiO_2 consisting of a network of corner sharing tetrahedra. Hence, the experimental infrared spectra do not seem to contain features which point to the presence of any kind of structural irregularity. We believe that the theoretical approach applied in this work will prove even more useful in interpreting infrared spectra of systems which present a larger degree of structural disorder than a-SiO_2.

We acknowledge the precious contribution of J. Sarnthein to previous projects, which have led to the present Letter. We also acknowledge clarifying discussions with A. Dal Corso and R. Resta. This work is partially supported by the Swiss National Science Foundation under Grant No. 20-49486.96. The calculations were performed on the NEC-SX4 of the Swiss Center for Scientific Computing (CSCS) in Manno.

[1] R. J. P. Lyon, Nature (London) **196**, 266 (1962).
[2] F. L. Galeener and G. Lucovsky, Phys. Rev. Lett. **37**, 1474 (1976).
[3] F. L. Galeener, A. J. Leadbetter, and M. W. Stringfellow, Phys. Rev. B **27**, 1052 (1983).
[4] B. Velde and R. Couty, J. Non-Cryst. Solids **94**, 238 (1987).
[5] C. T. Kirk, Phys. Rev. B **38**, 1255 (1988).
[6] R. M. Almeida, Phys. Rev. B **45**, 161 (1992).
[7] J. M. Carpenter and D. L. Price, Phys. Rev. Lett. **54**, 441 (1985).
[8] J. Sarnthein, A. Pasquarello, and R. Car, Science **275**, 1925 (1997).
[9] S. W. de Leeuw and M. F. Thorpe, Phys. Rev. Lett. **55**, 2879 (1985); M. F. Thorpe and S. W. de Leeuw, Phys. Rev. B **33**, 8490 (1986).
[10] V. N. Denisov *et al.*, J. Non-Cryst. Solids **64**, 195 (1984).
[11] P. F. McMillan, P. T. Poe, Ph. Gillet, and B. Reynard, Geochim. Cosmochim. Acta **58**, 3653 (1994).
[12] M. Wilson, P. A. Madden, M. Hemmati, and C. A. Angell, Phys. Rev. Lett. **77**, 4023 (1996).
[13] R. Resta, Rev. Mod. Phys. **66**, 899 (1994); *Berry Phase in Electronic Wavefunctions*, Troisième Cycle de la Physique en Suisse Romande, Lausanne, 1995–1996.
[14] L. V. Woodcock, C. A. Angell, and P. Cheeseman, J. Chem. Phys. **65**, 1565 (1976).
[15] R. J. Bell, P. Dean, and D. C. Hibbins-Butler, J. Phys. C **4**, 1214 (1971).
[16] Wei Jin, P. Vashishta, R. K. Kalia, J. P. Rino, Phys. Rev. B **48**, 9359 (1993).
[17] R. G. Della Valle and E. Venuti, Chem. Phys. **179**, 411 (1994).
[18] J. Sarnthein, A. Pasquarello, and R. Car, Phys. Rev. Lett. **74**, 4682 (1995); Phys. Rev. B **52**, 12 690 (1995).
[19] R. Car and M. Parrinello, Phys. Rev. Lett. **55**, 2471 (1985).
[20] A. Pasquarello *et al.*, Phys. Rev. Lett. **69**, 1982 (1992); K. Laasonen *et al.*, Phys. Rev. B **47**, 10 142 (1993).
[21] R. D. King-Smith and D. Vanderbilt, Phys. Rev. B **47**, 1651 (1993).
[22] We used the formulas given in J. P. Perdew and A. Zunger, Phys. Rev. B **23**, 5048 (1981).
[23] G. B. Bachelet, D. R. Hamann, and M. Schlüter, Phys. Rev. B **26**, 4199 (1982).
[24] D. Vanderbilt, Phys. Rev. B **41**, 7892 (1990).
[25] M. V. Berry, Proc. R. Soc. London A **392**, 45 (1984).
[26] W. Zhong, R. D. King-Smith, and D. Vanderbilt, Phys. Rev. Lett. **72**, 3618 (1994).
[27] Because of the use of ultrasoft PPs the Berry phase calculation must be generalized with respect to Refs. [13,21] by including an augmentation term.
[28] X. Gonze, D. C. Allan, and M. P. Teter, Phys. Rev. Lett. **68**, 3603 (1992); in *Phonon Scattering in Condensed Matter*, edited by M. Meissner and R. O. Pohl (Springer-Verlag, Berlin, 1993), Vol. VII, p. 511.
[29] In a natural basis as defined in Ref. [28], the diagonal elements of the O charge tensor account on average for 99.28% of the norm, to be compared to 99.82% in α quartz [28].
[30] This recalls similar sum rules demonstrated for surfaces: A. Ruini, R. Resta, and S. Baroni (unpublished).
[31] P. Brüesh, in *Phonons: Theory and Experiments*, edited by P. Fulde (Springer-Verlag, Berlin, 1986), Vol. II, Chap. 2.
[32] P. N. Sen and M. F. Thorpe, Phys. Rev. B **15**, 4030 (1977).
[33] F. L. Galeener, Phys. Rev. B **19**, 4292 (1979).
[34] The $\mathbf{q} = 0$ limit is reached continuously and the depolarizing fields are in this way avoided [9].
[35] Anisotropic components are also important for LO-TO splittings in α quartz [28].